Journal of Biomechanics 60 (2017) 261–265

Contents lists available at ScienceDirect

Journal of Biomechanics

journal homepage: www.elsevier.com/locate/jbiomech
www.JBiomech.com

Short communication

Real-time observation of fluid flows in tissue during stress relaxation using Raman spectroscopy

Maria Parkes *, Philippa Cann, Jonathan Jeffers

Imperial College London, London, United Kingdom

ARTICLE INFO

Article history:
Accepted 13 June 2017

Keywords:
Cartilage
In-situ Raman
Compression testing

ABSTRACT

This paper outlines a technique to measure fluid levels in articular cartilage tissue during an unconfined stress relaxation test. A time series of Raman spectrum were recorded during relaxation and the changes in the specific Raman spectral bands assigned to water and protein were monitored to determine the fluid content of the tissue. After 1000 s unconfined compression the fluid content of the tissue is reduced by an average of 3.9% ± 1.7%. The reduction in fluid content during compression varies between samples but does not significantly increase with increasing strain. Further development of this technique will allow mapping of fluid distribution and flows during dynamic testing making it a powerful tool to understand the role of interstitial fluid in the functional performance of cartilage.

1. Introduction

Articular cartilage is a biphasic tissue, containing around 80% interstitial fluid. The flow and distribution of this fluid in the tissue during dynamic loading is important in resisting load, in providing the exceptionally low friction levels found at the articular surfaces and in providing nutrients and mechanical stimuli to the cartilage cells (Ateshian, 2009; Grad et al., 2011; Mow et al., 1984). Similarly fluid flows in bioreactors increase collagen production, chondrocyte viability, and the 3-D structure and tensile modulus of engineered tissue (Gemmiti and Guldberg, 2006; Vunjak-Novakovic et al., 1999; Wartella and Wayne, 2009). Understanding these flows is then crucial in our continuing quest to regrow damaged cartilage and to develop biomimetic bearings.

The prediction of fluid flows during compression has been performed in finite element (FE) models. However, the predicted flows are dependent on such variables as inclusion and orientation of collagen fibrils (Federico and Herzog, 2008), the tension-compression parameters (Soltz and Ateshian, 2000a; Wilson et al., 2005) and the specified permeability of the solid matrix (Lai et al., 1981). Some validation of FE models has been achieved through real-time measurements of fluid pressure in a compression test (Soltz and Ateshian, 2000b). However these are general measurements over the bulk volume of the cartilage and do not allow spatial variations in pressure or fluid flow to be determined.

Spatial variation in diffusion coefficients as well as the directional diffusion of water in cartilage have been measured using Magnetic Resonance imaging (MRi) under static conditions (Pierce et al., 2010; Xia et al., 1994). Whilst MRi offers the spatial resolution needed to measure fluid flow, acquisition times in the order of minutes prevent this technique from being used for real-time measurements (Binks et al., 2013).

Here we detail a new technique which allows the measurement of changes in fluid distribution in cartilage with both spatial and temporal resolution. Our technique uses confocal Raman spectroscopy measurements during an unconfined compression test. This technique has spatial resolution of less than 1 μm in the *x*-*y* plane and approximately 7 μm in the *z*-plane, and individual measurements are performed at a frequency of 10 Hz. Whilst this initial testing has been performed on osteochondral plugs the method could be extended to other tissues.

2. Methods

Osteochondral samples ($n = 8$) were obtained using an 8 mm biopsy punch from porcine femoral condyles, and frozen at −20 °C until required. Cartilage thickness after thawing was determined optically. Samples were mounted in polyethylene holders using bone cement which was cured for 1 h. Two points approximately 1 mm apart were marked on the cartilage surface with a needle dipped in Indian ink to locate the measurement area. The PE holders were press fit into a petri dish mounted on the compression stage. Throughout measurements samples were kept immersed in phosphate buffered saline.

* Corresponding author at: Department of Mechanical Engineering, Imperial College London, London SW7 2AZ, United Kingdom.

E-mail addresses: maria.parkes04@imperial.ac.uk (M. Parkes), p.cann@imperial.ac.uk (P. Cann), j.jeffers@imperial.ac.uk (J. Jeffers).

http://dx.doi.org/10.1016/j.jbiomech.2017.06.004
0021-9290/

A custom loading device was used, driven by a linear actuator with a linear travel per step of 3 μm. Loads were recorded by a 6 axis load cell, with an axial resolution of 1/80 N (Gamma, ATI Industrial Automation, USA). The cartilage samples were compressed against a 40 mm diameter glass plate that was held fixed in space (Fig. 1).

Raman spectra were collected using an Alpha300R, confocal Raman spectrometer (WITec Gmbh, Ulm, Germany) using a laser wavelength of 532 nm, a 20x objective and a 100 μm pinhole giving an axial resolution of 7 μm. Spectra were recorded at the interface between the glass plate and the cartilage sample during compression with an integration time of 0.1 s.

2.1. Unconfined compression

For all samples two unconfined compression test lasting 20 min were performed, with 24 h recovery at 4 °C between tests. A pre-load of 0.5 N was applied to ensure contact with the cartilage surface. Contact was confirmed by acquisition of a single Raman spectra at the glass-cartilage interface. The sample was then allowed to relax for 10 min under pre-load before the stress relaxation step was started. The sample was loaded to either 10% or 20% strain at 1% strain per second. The strain was held constant for 20 min and the reaction force recorded. Simultaneously a continuous time series of 10,000 Raman spectra were acquired.

2.2. Strain recovery

For three samples a further test was conducted to determine if the proposed technique would accurately measure water content during strain recovery. As before a pre-load of 0.5 N was applied with 10 min rest before the sample was loaded to 10% compression. The position was held constant for 1000 s, the sample was then unloaded by returning the loading device to its original position at 0% strain. A time series of 15,000 Raman spectra were acquired throughout the process.

2.3. Calculation of water content

The ratio of water to protein content in the cartilage tissue was determined using the ratio of intensities of the Raman peaks at 3390 cm^{-1} due to OH stretching vibrations in water and 2935 cm^{-1} due to CH_3 stretching vibrations in proteins. This method has previously been used to determine water content in eye lenses and skin tissue (Caspers, 2003; Siebinga et al., 1991). Matlab (MATLAB and Statistics Toolbox Release 2015a, The MathWorks Inc., Natick, Massachusetts) was used to process all data. To correct for fluorescence background a 1st order baseline was fit between the spectral points of 2500 and 3800 cm^{-1}. The intensity of the water peak was calculated as the sum intensity between 3350 and 3550 and the protein peak as the sum intensity between 2910–2965 cm^{-1}. To calculate the water content the following equations as proposed in (Caspers, 2003) were used:

$$\frac{W}{P} = \frac{m_w}{m_p} \cdot R \tag{1}$$

$$\text{Water content } (\%) = \frac{m_w}{m_w + m_p} = \frac{\frac{W}{P}}{\frac{W}{P} + R} \cdot 100\% \tag{2}$$

where W is the integrated Raman signal of water, P is the integrated Raman signal of protein, m_w and m_p are the mass of water and protein respectively and R is a proportionality constant representing the water:protein signals in solutions of

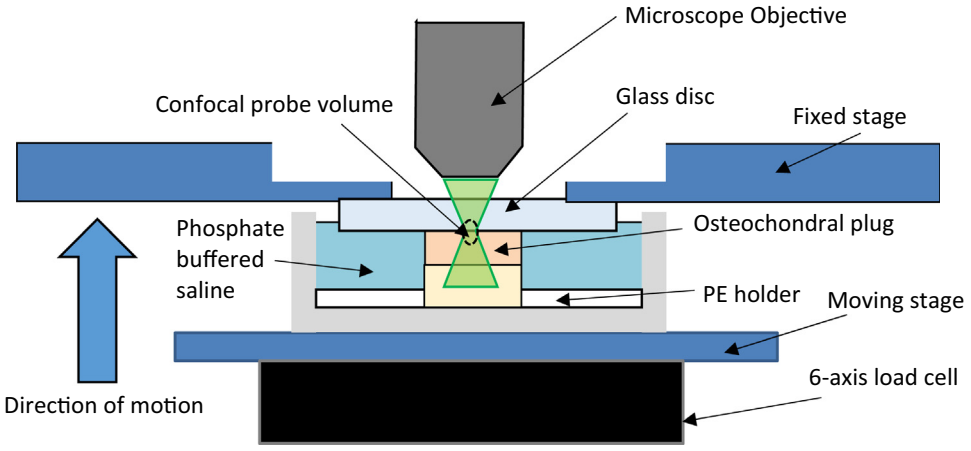

Fig. 1. Schematic of loading rig.

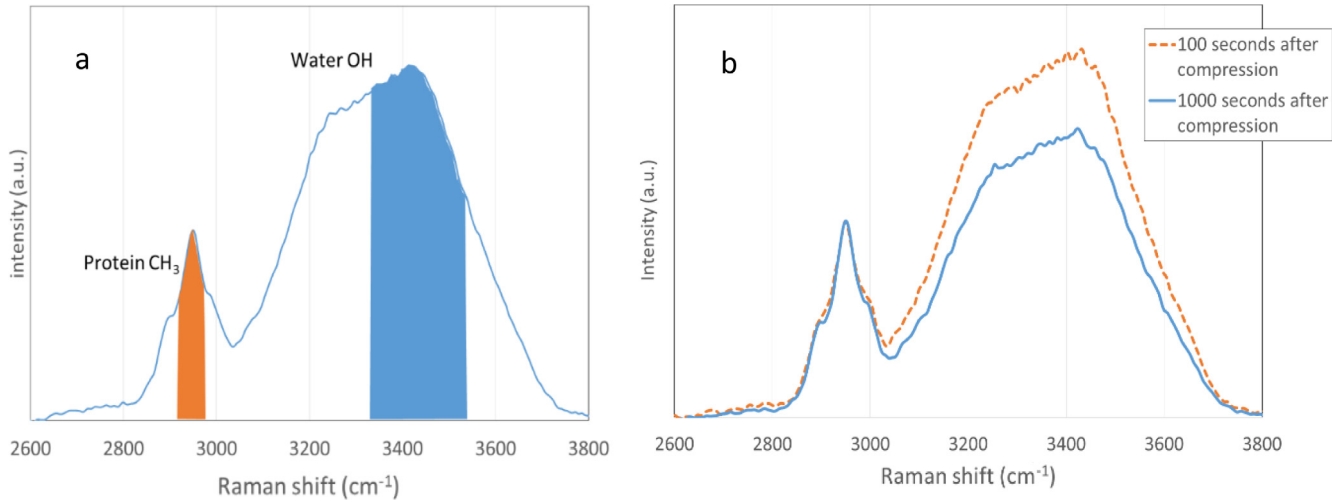

Fig. 2. Typical Raman spectra for cartilage sample recorded (a) under 0.5 N pre-load showing areas used to calculate water and protein content (b) at 100 and 1000 s after compression showing changes in peak ratio.

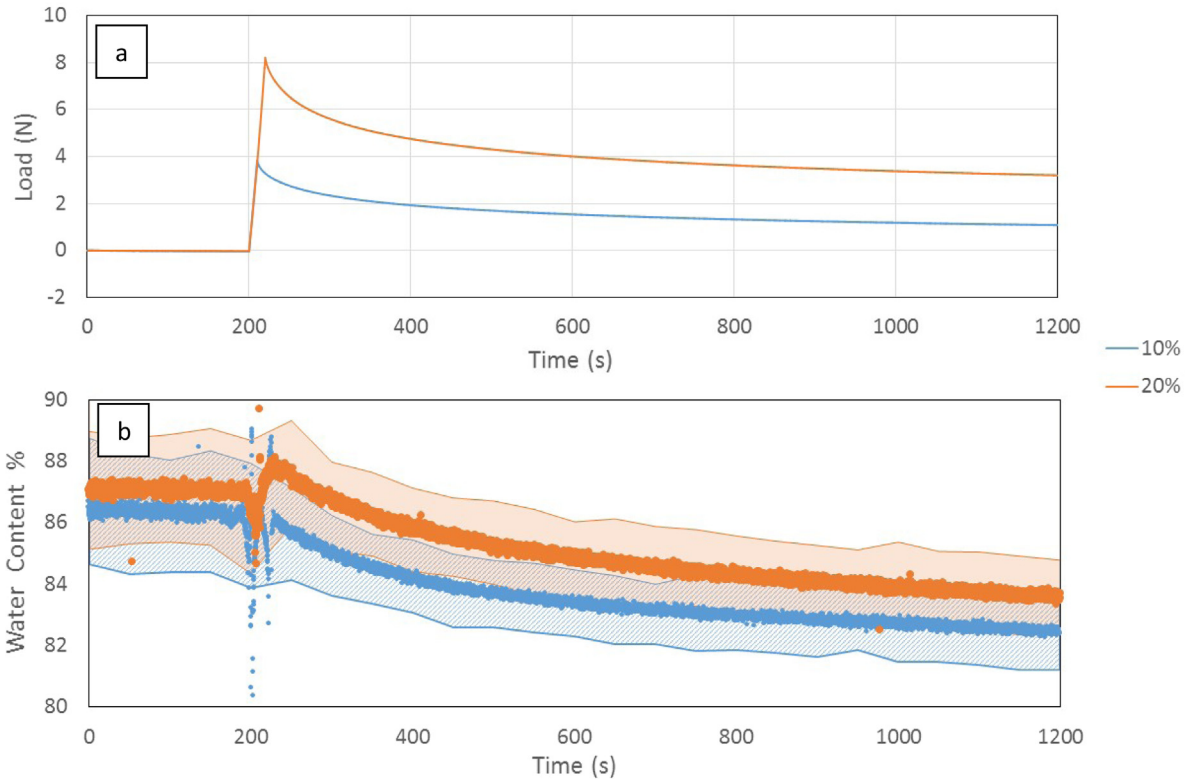

Fig. 3. Average results for 8 samples showing (a) stress relaxation curve (b) simultaneous water content calculated from water:protein ratio at 10 and 20% compression with bands showing 95% confidence intervals.

known concentration. For this system we determined R to be 1.14 using solutions of Bovine Serum Albumin in water, a little lower than the previously reported range of 2.0 ± 0.3 (Caspers, 2003).

3. Results

Typical Raman spectra for the cartilage after pre-loading the cartilage to 0.5 N and following compression are shown in Fig. 2. The average load during the unconfined compression test is shown in Fig. 3a. The load carried by the cartilage increases rapidly during the compression phase and then reduces during the relaxation phase. This relaxation is attributed to the drop in fluid pressure as fluid flows out of the compressed tissue but also the flow independent reorganisation of the collagen structure (June and Fyhrie, 2013).

The simultaneous measurement of the water:protein ratio is shown in Fig. 3b. Before compression the average water content of the cartilage tissue was 86.4% ± 2.8 for the 10% group and 87.1% ± 2.5 for the 20% group consistent with the expected water content of 80% for the superficial zone of articular cartilage (Sophia Fox et al., 2009). At 10% compression this dropped to 82.4% ± 1.7 and at 20% compression to 83.4% ± 1.8. Fig. 3b also shows that the rate of reduction in water content decreases with time.

The percentage reduction of fluid content shows some correlation with the initial water content of each sample (Fig. 4). This indicates that for a sample that is originally more hydrated there is more fluid that can be released from the sample.

The average change in fluid content for 3 samples during compression and then following unloading is shown in Fig. 5. Directly after unloading the water content reaches close to 100%. This suggests that the cartilage remains compressed and the gap between the cartilage surface and the glass plate is filled with water. As the cartilage recovers the gap between the plate and the cartilage reduces and the water content drops, until the cartilage is fully recovered and the measured water content returns to the pre-compression value.

4. Discussion

Using confocal Raman spectroscopy we have shown it is possible to directly measure the changes in fluid content of cartilage tissue during an unconfined compression test. Real-time measurements allow the instantaneous fluid content of the tissue to be determined as well as showing changes in the rate of fluid flow. Strain recovery tests have shown that this technique can also

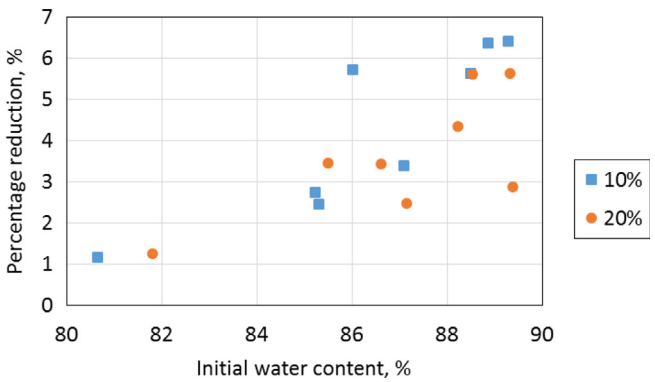

Fig. 4. The reduction in water content for all samples compared with the initial water content before compression.

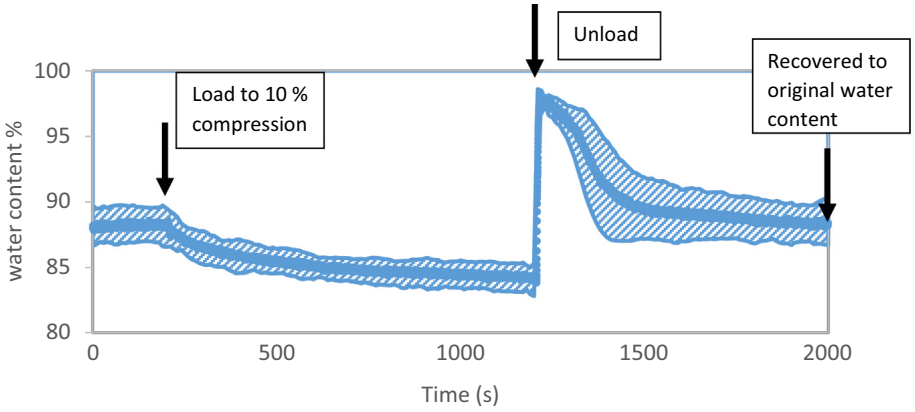

Fig. 5. Water content calculated from water:protein ratio at 10% compression and following unloading showing gradual recovery back to original level of water content with bands showing 95% confidence interval.

be used to measure the rate of fluid uptake by cartilage during free swelling.

Following compression we saw a reduction in water content of around 4%. Other authors have used MRi to show a water content reduction of around 2% in vivo in patella cartilage following compression of the cartilage during knee bends (Liess et al., 2002). We would expect to see a higher reduction here due to the exposed edge of the osteochondral plug where free draining can occur and a higher level of compression than seen in physiological activities (Liess et al., 2002).

With the increase from 10 to 20% compression there is an associated increase in loading and hence fluid pressure. Despite this there is a similar reduction in fluid content for both conditions. Darcy's Law for fluid flow in a porous medium relates the volumetric discharge, Q to the pressure, P and permeability κ such that:

$$Q = \frac{-\kappa A}{\eta}\frac{\Delta P}{l} \tag{3}$$

where η is the fluid viscosity, A is the cross-sectional area and l is the length of the measured volume. As our probe volume and fluid viscosity are constant, if the pressure increases but the volumetric discharge is the same then the permeability must decrease with compression. This is in agreement with results from *in silico* (Guo et al., 2015) and *in vitro* (Reynaud and Quinn, 2006) tests.

An alternative explanation of why there is no measured increase in fluid flow with increased compression may be found in the anisotropic structure of cartilage, that results in depth dependent properties (Chen et al., 2001). During compression the surface zone initially experiences a higher strain and fluid pressure than tissue at a greater distance from the cartilage surface (Wang et al., 2001). With increasing compression the fluid in the middle and deep zones of the cartilage becomes pressurised leading to fluid flow and increasing strain in these zones (Wang et al., 2001). The technique described here probes only a localised volume of tissue at the cartilage surface and so would not measure any increased fluid flow in the deeper tissue zones that occurs with the increase of overall cartilage strain.

By comparing the reduction in water content for each sample with the initial value we found that more hydrated tissues released more water. Similar results have been found for osteoarthritic cartilage which tends to be more hydrated than healthy cartilage (Setton et al., 1999).

The strain recovery tests have shown that following unloading swelling of the cartilage takes place over a timeframe of around 15 min. The rate of swelling is highest just after unloading and reduces as the cartilage recovers its initial volume. The final fluid content is within 0.4% of that measured pre-compression. The precision of this value is strong evidence that the technique measures actual changes in water content rather than some experimental artefact.

Here we have made measurements at one location per sample. By showing a reduction in water content we are showing a flow of water out of the measured probe volume, however this could also be observed with measurements before and after loading. We also show that the rate of fluid flow changes with time with an observable reduction occurring over a timescale of seconds. This would not be measurable without real-time measurements. To determine the pattern of fluid flow through the cartilage a series of measurements at different locations would need to be made.

Raman spectroscopy has been shown to be a useful tool to map the structure, measure early degeneration and collagen stretching in cartilage (Bonifacio et al., 2010; Lim et al., 2011; Wang et al., 2000). This previous work has examined the tissue under static conditions. Here we have shown that Raman spectroscopy can also be used to understand chemical changes during dynamic testing with high temporal resolution. This technique allows us to observe changes in tissue properties such as water content and permeability occurring under the dynamic conditions experienced during daily activities.

Conflict of interest statement

The authors have no conflicts of interest to declare.

Acknowledgments

This study was supported by EPSRC [EP/K027549/1].

References

Ateshian, G.A., 2009. The role of interstitial fluid pressurization in articular cartilage lubrication. J. Biomech. 42, 1163–1176. http://dx.doi.org/10.1016/j.jbiomech.2009.04.040.

Binks, D.A., Hodgson, R.J., Ries, M.E., Foster, R.J., Smye, W., McGonagle, D., Radjenovic, A., 2013. Quantitative parametric MRI of articular cartilage: a review of progress and open challenges. Br. J. Radiol. 86. http://dx.doi.org/10.1259/bjr.20120163.

Bonifacio, A., Beleites, C., Vittur, F., Marsich, E., Semeraro, S., Paoletti, S., Sergo, V., 2010. Chemical imaging of articular cartilage sections with Raman mapping, employing uni- and multi-variate methods for data analysis. Analyst 135, 3193–3204. http://dx.doi.org/10.1039/c0an00459f.

Caspers, P., 2003. In Vivo Skin Characterization by Confocal Raman Microspectroscopy. Erasmus University Rotterdam.

Chen, A.C., Bae, W.C., Schinagl, R.M., Sah, R.L., 2001. Depth-and strain-dependent mechanical and electromechanical properties of full-thickness bovine articular

cartilage in con“ned compression. J. Biomech. 34, 1–12. http://dx.doi.org/10.1016/S0021-9290(00)00170-6.
Federico, S., Herzog, W., 2008. On the anisotropy and inhomogeneity of permeability in articular cartilage. Biomech. Model. Mechanobiol. 7, 367–378. http://dx.doi.org/10.1007/s10237-007-0091-0.
Gemmiti, C.V., Guldberg, R.E., 2006. Fluid flow increases type II collagen deposition and tensile mechanical properties in bioreactor-grown tissue-engineered cartilage. Tissue Eng. 12, 469–479. http://dx.doi.org/10.1089/ten.2006.12.469.
Grad, S., Eglin, D., Alini, M., Stoddart, M.J., 2011. Physical stimulation of chondrogenic cells in vitro: a review. Clin. Orthop. Relat. Res. 469, 2764–2772. http://dx.doi.org/10.1007/s11999-011-1819-9.
Guo, H., Maher, S.A., Torzilli, P.A., 2015. A biphasic finite element study on the role of the articular cartilage superficial zone in confined compression. J. Biomech. 48, 166–170. http://dx.doi.org/10.1016/j.jbiomech.2014.11.007.A.
June, R.K., Fyhrie, D.P., 2013. A comparison of cartilage stress-relaxation models in unconfined compression: QLV and stretched exponential in combination with fluid flow. Comput. Methods Biomech. Biomed. Eng. 16, 565–576. http://dx.doi.org/10.1080/10255842.2011.629612.
Lai, W.M., Mow, V.C., Roth, V., 1981. Effects of nonlinear strain-dependent permeability and rate of compression on the stress behavior of articular cartilage. J. Biomech. Eng. 103, 61–66. http://dx.doi.org/10.1115/1.3138261.
Liess, C., Lüsse, S., Karger, N., Heller, M., Glüer, C.G., 2002. Detection of changes in cartilage water content using MRI T2-mapping in vivo. Osteoarthr. Cartil. 10, 907–913. http://dx.doi.org/10.1053/joca.2002.0847.
Lim, N.S.J., Hamed, Z., Yeow, C.H., Chan, C., Huang, Z., 2011. Early detection of biomolecular changes in disrupted porcine cartilage using polarized Raman spectroscopy. J. Biomed. Opt. 16, 17003. http://dx.doi.org/10.1117/1.3528006.
Mow, V., Holmes, M., Lai, W.M., 1984. Fluid transport and mechanical properties of articular cartilage: a review. J. Biomech. 17, 377–394.
Pierce, D.M., Trobin, W., Raya, J.G., Trattnig, S., Bischof, H., Glaser, C., Holzapfel, G.A., 2010. DT-MRI based computation of collagen fiber deformation in human articular cartilage: a feasibility study. Ann. Biomed. Eng. 38, 2447–2463. http://dx.doi.org/10.1007/s10439-010-9990-9.
Reynaud, B., Quinn, T.M., 2006. Anisotropic hydraulic permeability in compressed articular cartilage. J. Biomech. 39, 131–137. http://dx.doi.org/10.1016/j.jbiomech.2004.10.015.
Setton, L.A., Elliott, D.M., Mow, V.C., 1999. Altered mechanics of cartilage with osteoarthritis: human osteoarthritis and an experimental model of joint degeneration. Osteoarthr. Cartil. 7, 2–14. http://dx.doi.org/10.1053/joca.1998.0170.
Siebinga, I., Vrensen, G.F., De Mul, F.F., Greve, J., 1991. Age-related changes in local water and protein content of human eye lenses measured by Raman microspectroscopy. Exp. Eye Res. 53, 233–239.
Soltz, M.A., Ateshian, G.A., 2000a. A conewise linear elasticity nonlinearity in articular cartilage. Bioengineering 122.
Soltz, M.A., Ateshian, G.A., 2000b. Interstitial fluid pressurization during confined compression cyclical loading of articular cartilage. Ann. Biomed. Eng. 28, 150–159.
Sophia Fox, A.J., Bedi, A., Rodeo, S.A., 2009. The basic science of articular cartilage: structure, composition, and function. Sports Health 1, 461–468. http://dx.doi.org/10.1177/1941738109350438.
Vunjak-Novakovic, G., Martin, I., Obradovic, B., Treppo, S., Grodzinsky, A.J., Langer, R., Freed, L.E., 1999. Bioreactor cultivation conditions modulate the composition and mechanical properties of tissue-engineered cartilage. J. Orthop. Res. 17, 130–138. http://dx.doi.org/10.1002/jor.1100170119.
Wang, C.C.B., Hung, C.T., Mow, V.C., 2001. An analysis of the effects of depth-dependent aggregate modulus on articular cartilage stress-relaxation behavior in compression. J. Biomech. 34, 75–84. http://dx.doi.org/10.1016/S0021-9290(00)00137-8.
Wang, Y.N., Galiotis, C., Bader, D.L., 2000. Determination of molecular changes in soft tissues under strain using laser Raman microscopy. J. Biomech. 33, 483–486. http://dx.doi.org/10.1016/S0021-9290(99)00194-3.
Wartella, K.A., Wayne, J.S., 2009. Bioreactor for biaxial mechanical stimulation to tissue engineered constructs. J. Biomech. Eng. 131, 44501. http://dx.doi.org/10.1115/1.3049859.
Wilson, W., Van Donkelaar, C.C., Van Rietbergen, R., Huiskes, R., 2005. The role of computational models in the search for the mechanical behavior and damage mechanisms of articular cartilage. Med. Eng. Phys. 27, 810–826. http://dx.doi.org/10.1016/j.medengphy.2005.03.004.
Xia, Y., Farquhar, T., Burton-Wurster, N., Ray, E., Jelinski, L.W., 1994. Diffusion and relaxation mapping of cartilage-bone plugs and excised disks using microscopic magnetic resonance imaging. Magn. Reson. Med. 31, 273–282. http://dx.doi.org/10.1002/mrm.1910310306.